Chinese Chemical Letters 36 (2025) 110102

Contents lists available at ScienceDirect

Chinese Chemical Letters

journal homepage: www.elsevier.com/locate/cclet

Near-perfect separation of alicyclic ketones and alicyclic alcohols by nonporous adaptive crystals of perethylated pillar[5]arene and pillar[6]arene

Jingyu Chen[1], Sha Wu[1], Yuhao Wang, Jiong Zhou*

Department of Chemistry, College of Sciences, Northeastern University, Shenyang 110819, China

ARTICLE INFO

Article history:
Received 19 March 2024
Revised 22 May 2024
Accepted 6 June 2024
Available online 7 June 2024

Keywords:
Pillar[*n*]arenes
Nonporous adaptive crystals
Adsorptive separation
Host-guest complexes
Supramolecular chemistry

ABSTRACT

The separation of alicyclic ketones and alicyclic alcohols is one of the challenges in the field of petrochemical industry. However, traditional separation methods suffer from excessive energy consumption, complicated operation, and unsatisfactory separation efficiency for substances with similar boiling points. Herein, we offer an innovative method for the separation of alicyclic ketones and alicyclic alcohols employing nonporous adaptive crystals (NACs) of perethylated pillar[5]arene (EtP5) and perethylated pillar[6]arene (EtP6). NACs of EtP5 cannot adsorb either alicyclic ketones or alicyclic alcohols because of the small cavity size of EtP5. By contrast, NACs of EtP6 can separate cyclopentanone from the vapor mixture of cyclopentanone/cyclopentanol (v:v = 1:1) and cyclohexanone from the vapor mixture of cyclohexanone/cyclohexanol (v:v = 1:1) with purities of 99.1% and 100%, respectively. Density functional theory calculations show that the selectivity comes from the thermodynamic stability of the newly formed crystal structure after adsorption of the preferred guest molecule. Moreover, NACs of EtP6 can be reused without losing selectivity and performance.

Cyclopentanone (CPON) and cyclopentanol (CPOL) are vital raw materials for fine chemicals, which are widely used in the manufacture of new fragrances and pharmaceutical ingredients [1]. Additionally, CPON is also applied in biochemical research and the synthesis of insecticides and herbicides [2]. However, in the industrial production of CPON and CPOL, both compounds are often obtained simultaneously, necessitating efficient separation. Similarly, cyclohexanone (CHON) and cyclohexanol (CHOL) play a crucial role in the manufacture of adipamide, adipic acid, nylon-6, and nylon-66 [3]. Furthermore, CHON is used as an industrial solvent for resins, paints, dyes, and pesticides [4,5]. In industrial production, CHON and CHOL are inevitably obtained as mixtures [6–9]. At present, the main methods for separating CPOL/CPON or CHOL/CHON in industry include pressure-swing distillation, extractive distillation and membrane pervaporation [10]. However, subtle differences in structures and boiling points (CPOL: 413.95 K, CPON: 404.15 K; CHOL: 432.75 K, CHON: 428.15 K) prevent them from being separated by traditional distillation, and there are many problems such as high energy consumption, low utilization rate of raw materials, and serious environmental pollution [11]. Thus, the development of energy-efficient separation techniques is imperative.

Taking use of the variations in molecular geometry and size, adsorptive separation *via* porous materials is an effective technique [12–14]. Porous materials such as zeolites, metal-organic frameworks (MOFs) and covalent organic frameworks (COFs) have been applied in adsorptive separation [15–25]. For example, MOFs have been used for gas adsorption and separation of harmful substances due to their high specific surface areas and ordered channels [26,27]. Nonetheless, the drawbacks of poor stability, intricate design requirements and elevated costs limit the extensive application of porous materials in industry [28–31]. Thus, it is still urgent to develop a kind of absorbent with stable structure and high selectivity.

Pillar[*n*]arenes were first reported in 2008 as a novel class of supramolecular hosts [32–37]. With the in-depth study of pillar[*n*]arenes, they have been applied in the fabrication of various supramolecular systems, including drug delivery systems, molecular machines, supramolecular polymers and supramolecular amphiphiles [38–48]. Recently, Huang and co-workers have innovatively proposed nonporous adaptive crystals (NACs) of pillar[*n*]arenes [49–51]. Different from traditional porous materials, NACs are nonporous in their original states. However, when suitable guest molecules are introduced, NACs can form internal and

* Corresponding author.
E-mail address: zhoujiong@mail.neu.edu.cn (J. Zhou).
[1] These authors contributed equally to this work.

https://doi.org/10.1016/j.cclet.2024.110102
1001-8417/

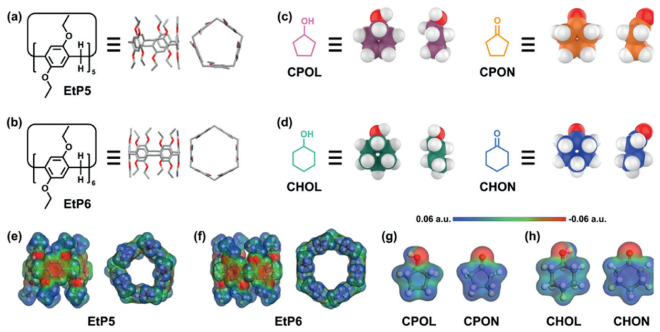

Fig. 1. Chemical structures of (a) perethylated pillar[5]arene (EtP5), (b) perethylated pillar[6]arene (EtP6), (c) cyclopentanol (CPOL) and cyclopentanone (CPON), (d) cyclohexanol (CHOL) and cyclohexanone (CHON). Electrostatic potential maps of (e) EtP5, (f) EtP6, (g) CPOL and CPON, (h) CHOL and CHON.

external pores, which result in excellent adsorption performances [52–56]. Besides, NACs have the advantages of good thermal stability, easy preparation and moisture resistance [57–60]. Based on these unique features, NACs of pillar[*n*]arenes can be used to separate important chemical feedstocks with high selectivities [61–64]. However, pillar[*n*]arenes-based NACs have never been used for the separation of alicyclic ketones and alicyclic alcohols.

Herein, for the first time, NACs of perethylated pillar[5]arene (EtP5) and perethylated pillar[6]arene (EtP6) were used as adsorptive materials to separate CPON from the mixture of CPOL/CPON as well as CHON from the mixture of CHOL/CHON (Figs. 1a–d). NACs of EtP5 (EtP5α) could adsorb neither alicyclic ketones nor alicyclic alcohols because of the small cavity size of EtP5 (Table S1 in Supporting information). By contrast, NACs of EtP6 (EtP6β) separated CPON from an equal-volume mixture of CPOL and CPON, as well as CHON from an equal-volume mixture of CHOL and CHON, with purities of 99.1% and 100%, respectively. Density functional theory calculations revealed that the near-perfect selectivity originated from the thermodynamic stability of the new host-guest crystal structure of EtP6β upon capturing the preferred guest. Furthermore, the removal of CPON and CHON transformed the host-guest complex back to EtP6β, making EtP6β highly recyclable.

The activated EtP5 (EtP5α) and EtP6 (EtP6β) as adsorptive separation materials were prepared according to the previously reported procedure [65]. ^{1}H NMR (Figs. S1 and S2 in Supporting information) and thermogravimetric analyses (TGA, Figs. S3 and S4 in Supporting information) proved that the solvent was removed. Powder X-ray diffraction (PXRD, Figs. S5 and S6 in Supporting information) showed that both EtP5α and EtP6β were crystalline.

ESP maps of EtP5, EtP6, CPOL, CPON, CHOL and CHON were calculated to analyze the possibility of complexation behaviors. ESP maps revealed that the cavities of EtP5 and EtP6 exhibited strong electro-negativity due to the electron-rich 1,4-diethoxybenzene units (Figs. 1e and f). Moreover, the alicyclic areas of CPON and CHON displayed stronger electro-positivity than those of CPOL and CHOL since the electron-withdrawing effect of the carbonyl group was greater than that of the hydroxyl group (Figs. 1g and h). These results indicated that CPON and CHON had the potential to form host-guest complexes with EtP5 and EtP6.

According to the results of the ESP map surface measurements, the adsorption capacities of EtP5α and EtP6β towards single-component CPOL and CPON vapors were explored. EtP5α took up negligible amounts of CPOL and CPON vapors, which was confirmed by ^{1}H NMR spectra (Fig. 2a, Figs. S7 and S8 in Supporting information). But for EtP6β, time-dependent solid-vapor sorption experiments demonstrated their capacities to adsorb CPOL and CPON vapors. The uptake of CPOL vapor by EtP6β was negligible (Figs. S9 and S11 in Supporting information). However, after

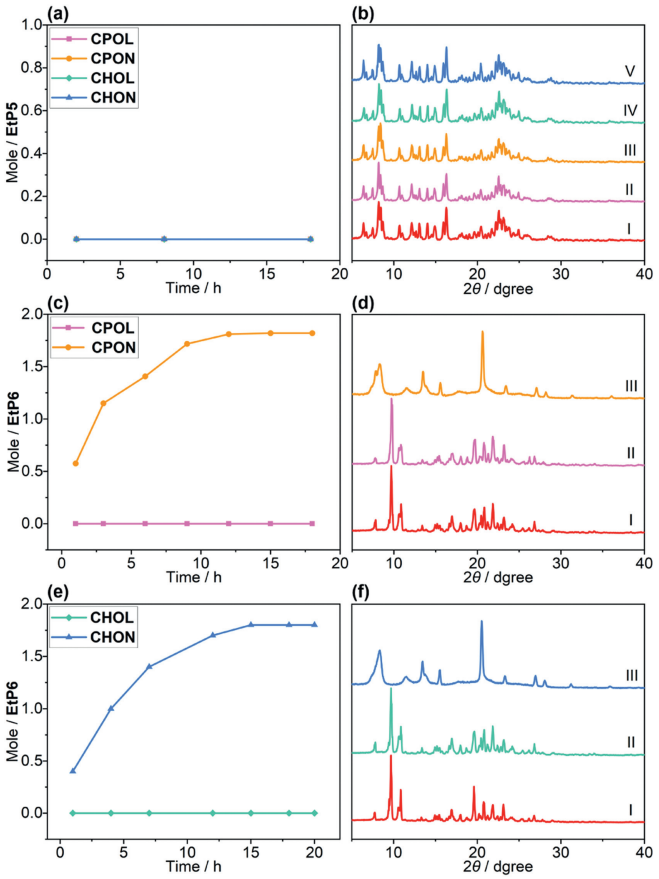

Fig. 2. (a) Time-dependent solid-vapor sorption plots of EtP5α for single-component CPOL, CPON, CHOL and CHON vapors. (b) PXRD patterns of EtP5α: (I) original EtP5α; (II) after adsorption of CPOL vapor; (III) after adsorption of CPON vapor; (IV) after adsorption of CHOL vapor; (V) after adsorption of CHON vapor. (c) Time-dependent solid-vapor sorption plots of EtP6β for single-component CPOL and CPON vapors. (d) PXRD patterns of EtP6β: (I) original EtP6β; (II) after adsorption of CPOL vapor; (III) after adsorption of CPON vapor. (e) Time-dependent solid-vapor sorption plots of EtP6β for single-component CHOL and CHON vapors. (f) PXRD patterns of EtP6β: (I) original EtP6β; (II) after adsorption of CHOL vapor; (III) after adsorption of CHON vapor.

12 h, EtP6β reached the saturation point for adsorbing CPON vapor (Figs. S10 and S12 in Supporting information). As calculated from ^{1}H NMR spectra, the amount of CPON adsorbed by EtP6β was about two CPON molecules per EtP6 (Fig. 2c). TGA further confirmed the adsorption and storage of CPON by EtP6β (Figs. S13 and S14 in Supporting information). The TGA result of EtP6β after adsorption of CPON vapor showed a weight loss of 12.5% at 90 °C, indicating that one EtP6 molecule absorbed two CPON molecules.

Similarly, the adsorption capacities of EtP5α and EtP6β for single-component CHOL and CHON vapors were investigated. For EtP5α, the uptake of CHOL and CHON vapors was negligible (Fig. 2a, Figs. S15 and S16 in Supporting information). As for EtP6β, according to ^{1}H NMR spectra, it took about 15 h to reach the saturation point for adsorbing CHON vapor, and the uptake amount of CHON could be calculated to be two CHON molecules per EtP6 molecule, while the uptake of CHOL vapor was negligible (Fig. 2e, Figs. S17–S20 in Supporting information). Moreover, the TGA result of EtP6β after adsorption of CHON vapor showed a weight loss of 14.3% at 90 °C, indicating that one EtP6 molecule absorbed two CHON molecules (Figs. S21 and S22 in Supporting information).

Powder X-ray diffraction (PXRD) experiments were carried out to investigate the structures of EtP5α and EtP6β upon the uptake of single-component CPOL, CPON, CHOL and CHON vapors.

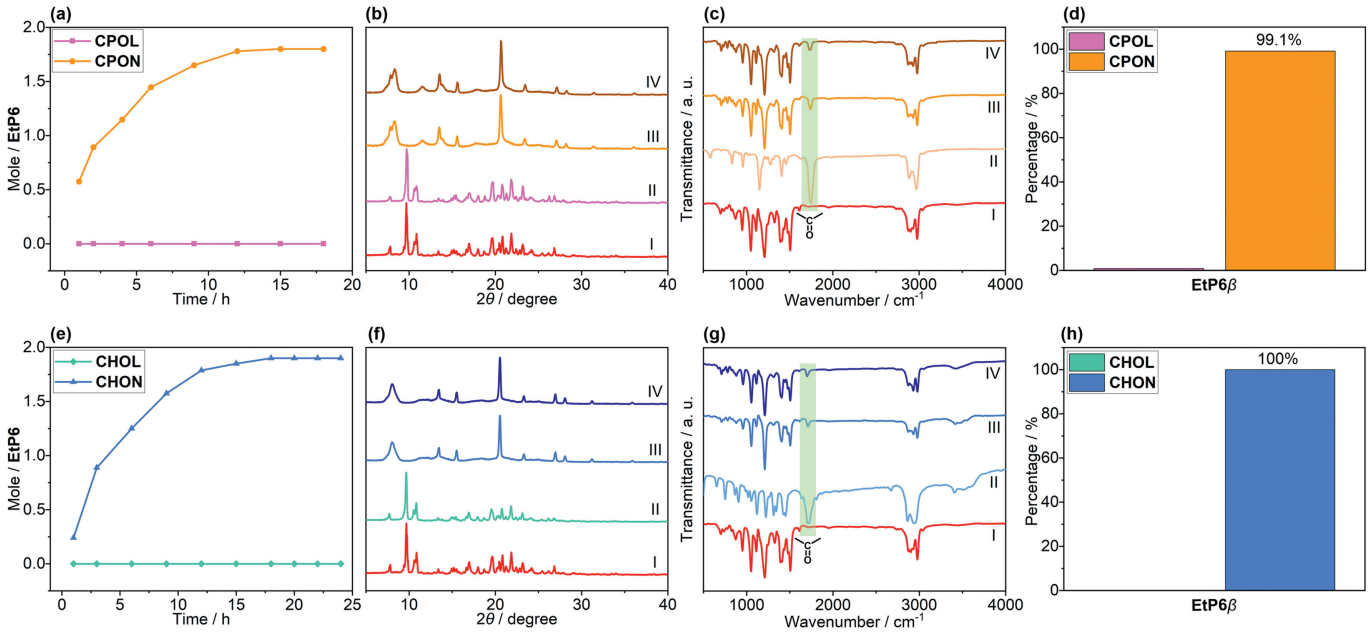

Fig. 3. (a) Time-dependent solid-vapor sorption plots of EtP6β for the vapor mixture of CPOL and CPON (v:v = 1:1). (b) PXRD patterns of EtP6β: (I) original EtP6β; (II) after adsorption of CPOL vapor; (III) after adsorption of CPON vapor; (IV) after adsorption of the vapor mixture of CPOL and CPON (v:v = 1:1). (c) FT-IR spectra of: (I) original EtP6β; (II) CPON; (III) EtP6β after adsorption of CPON vapor; (IV) EtP6β after adsorption of the vapor mixture of CPOL and CPON (v:v = 1:1). (d) Relative amounts of CPOL and CPON adsorbed by EtP6β after 12 h as measured by HS-GC. (e) Time-dependent solid-vapor sorption plots of EtP6β for the vapor mixture of CHOL and CHON (v:v = 1:1). (f) PXRD patterns of EtP6β: (I) original EtP6β; (II) after adsorption of CHOL vapor; (III) after adsorption of CHON vapor; (IV) after adsorption of the vapor mixture of CHOL and CHON (v:v = 1:1). (g) FT-IR spectra of: (I) original EtP6β; (II) CHON; (III) EtP6β after adsorption of CHON vapor; (IV) EtP6β after adsorption of the vapor mixture of CHOL and CHON (v:v = 1:1). (h) Relative amounts of CHOL and CHON adsorbed by EtP6β after 16 h as measured by HS-GC.

The PXRD patterns of EtP5α did not change after the uptake of single-component CPOL, CPON, CHOL and CHON vapors (Fig. 2b), which further confirmed that EtP5α had no adsorption capacity for CPOL, CPON, CHOL and CHON vapors. The PXRD patterns of EtP6β changed after the uptake of CPON and CHON vapors, implying that the uptake of CPON and CHON vapors by EtP6β induced the formation of new structures (Figs. 2d and f, Figs. S24 and S26 in Supporting information). However, the PXRD patterns of EtP6β did not change after the adsorption of CPOL or CHOL vapor, indicating that the structure of EtP6β did not change after exposure to CPOL or CHOL vapor (Figs. S23 and S25 in Supporting information).

Inspired by the adsorption capabilities of EtP6β for CPON and CHON vapors in single-component adsorption experiments, we further investigated the selective adsorption capabilities of EtP6β for the vapor mixture of CPOL and CPON (v:v = 1:1) and the vapor mixture of CHOL and CHON (v:v = 1:1). For the vapor mixture of CPOL and CPON, the uptake of CPON vapor by EtP6β increased over time and reached a saturation point after 12 h, while the adsorption of CPOL vapor was almost negligible (Fig. 3a). The adsorption amount of CPON vapor was close to two CPON molecules per EtP6 (Figs. S27 and S28 in Supporting information). In addition, the PXRD pattern of EtP6β after exposure to the vapor mixture of CPOL and CPON matched well with that of EtP6β after exposure to CPON vapor alone (Fig. 3b and Fig. S29 in Supporting information).

Fourier transform infrared (FT-IR) was also used to investigate the selectivity of EtP6β. The FT-IR spectrum of CPOL showed a typical stretching vibration peak associated with the -OH group of CPOL at 3400 cm^{-1}. However, the -OH peak in the spectrum of EtP6β after the uptake of CPOL vapor was not found (Fig. S30 in Supporting information). The C=O peak in the FT-IR spectrum of EtP6β after the uptake of CPON vapor was observed, which was associated with the C=O group of CPON at 1705 cm^{-1} (Fig. S31 in Supporting information). Additionally, the stretching vibration peak of the C=O group was also observed in the FT-IR spectrum of EtP6β after adsorption of the vapor mixture of CPOL and CPON (Fig. 3c). These results implied that EtP6β could selectively capture CPON vapor from the vapor mixture of CPOL and CPON.

Meanwhile, the potential of EtP6β to separate CHON from the vapor mixture of CHOL and CHON was studied. The CHON vapor adsorbed by EtP6β increased over time and reached the saturation point after 16 h (Fig. 3e). The adsorption amount of EtP6β for CHON vapor was calculated to be about two CHON molecules per EtP6, while the adsorption amount for CHOL vapor was negligible (Figs. S32 and S33 in Supporting information). Besides, the PXRD pattern of EtP6β upon exposure to the vapor mixture of CHOL and CHON was in accordance with that of EtP6β after exposure to CHON vapor alone (Fig. 3f and Fig. S34 in Supporting information). In addition, the stretching vibration peak of the C=O group on CHON was observed at 1705 cm^{-1} in the FT-IR spectrum of EtP6β after the adsorption of CHON vapor. However, there was no stretching vibration peak of -OH group on CHOL (3400 cm^{-1}) in the FT-IR spectrum of EtP6β after the adsorption of CHOL vapor (Figs. S35 and S36 in Supporting information). Moreover, the FT-IR spectrum of EtP6β after adsorption of the mixture vapor of CHOL and CHON showed a stretching vibration peak at 1705 cm^{-1} of CHON, but not at 3400 cm^{-1} of CHOL (Fig. 3g). These results indicated that EtP6β also exhibited selectivity towards CHON vapor.

Head space gas chromatography (HS-GC) experiment confirmed that CPON could be efficiently seperated from the vapor mixture of CPOL and CPON (v:v = 1:1) by EtP6β with a purity of 99.1% (Fig. 3d and Fig. S37 in Supporting information). Furthermore, HS-GC experiment also confirmed a 100% selectivity of EtP6β for CHON from the vapor mixture of CHOL and CHON (v:v = 1:1) (Fig. 3h and Fig. S38 in Supporting information). Therefore, compared with alicyclic alcohols, alicyclic ketones were more easily adsorbed and separated by EtP6β.

Various attempts have been made to obtain single crystals of guests-loaded EtP6, but failed. To further investigate the selectivity of EtP6β for CPON and CHON, the thermodynamics of host-guest complexes were calculated by density functional theory (DFT).

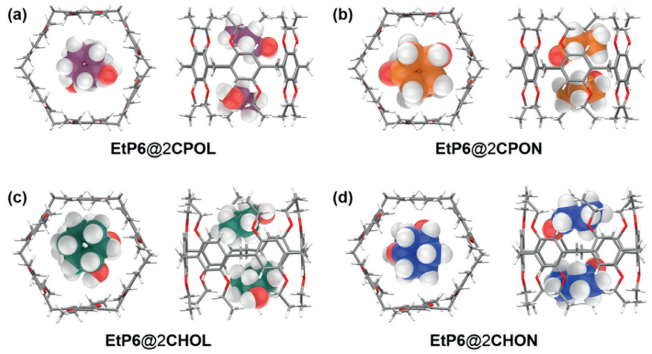

Fig. 4. Top and side views of DFT-optimized structures of (a) EtP6@2CPOL; (b) EtP6@2CPON; (c) EtP6@2CHOL; (d) EtP6@2CHON.

Table 1
Thermodynamic parameters of EtP6@2CPOL, EtP6@2CPON, EtP6@2CHOL and EtP6@2CHON at 298 K.

Sample	$\Delta H_{298}{}^{Sol}$ (kJ/mol)	$\Delta G_{298}{}^{Sol}$ (kJ/mol)
EtP6@2CPOL	−28.21	−4.01
EtP6@2CPON	−145.01	−72.21
EtP6@2CHOL	−38.12	−6.21
EtP6@2CHON	−147.22	−80.31

The structural models of CPOL-loaded EtP6 (EtP6@2CPOL), CPON-loaded EtP6 (EtP6@2CPON), CHOL-loaded EtP6 (EtP6@2CHOL), and CHON-loaded EtP6 (EtP6@2CHON) were established and optimized, respectively (Fig. 4). In these optimized structures, EtP6 tended to form 1:2 host-guest complexes with guests (CPOL, CPON, CHOL and CHON). Additionally, according to the orientation of guests entering the cavity of EtP6, CPOL, CPON, CHOL and CHON entered the cavity of EtP6 in a way that the alicyclic ring was parallel to the cavity plane.

Furthermore, the calculated energy values indicated that the formation of EtP6@2CPOL and EtP6@2CPON was thermodynamically feasible by $\Delta H_{298}{}^{Sol} = -28.21$ kJ/mol, $\Delta G_{298}{}^{Sol} = -4.01$ kJ/mol and $\Delta H_{298}{}^{Sol} = -145.01$ kJ/mol, $\Delta G_{298}{}^{Sol} = -72.21$ kJ/mol, respectively (Table 1). Compared with EtP6@2CPOL, EtP6@2CPON possessed a lower calculated energy value, indicating that the thermodynamic structure of EtP6@2CPON was more stable. Similarly, the calculated energy values of EtP6@2CHOL ($\Delta H_{298}{}^{Sol} = -38.12$ kJ/mol, $\Delta G_{298}{}^{Sol} = -37.92$ kJ/mol) were higher than those of EtP6@2CHON ($\Delta H_{298}{}^{Sol} = -147.22$ kJ/mol, $\Delta G_{298}{}^{Sol} = -80.31$ kJ/mol), which illustrated that the thermodynamic structure of EtP6@2CHON was more stable than that of EtP6@2CHOL (Table 1). These results revealed that the selectivity in the adsorption process arose from the thermodynamic stability of the host-guest complexes formed by EtP6 after loading guests.

Additionally, the structural models of CPOL-loaded EtP5 (EtP5@CPOL), CPON-loaded EtP5 (EtP5@CPON), CHOL-loaded EtP5 (EtP5@CHOL), and CHON-loaded EtP5 (EtP5@CHON) were also established and optimized to explain why EtP5α had no adsorption capacity for CPOL, CPON, CHOL, and CHON (Fig. 5). These guests were located in the cavity of EtP5 to form 1:1 host-guest complexes. Moreover, compared with EtP6@2CPON ($\Delta H_{298}{}^{Sol} = -145.01$ kJ/mol, $\Delta G_{298}{}^{Sol} = -72.21$ kJ/mol) and EtP6@2CHON ($\Delta H_{298}{}^{Sol} = -147.22$ kJ/mol, $\Delta G_{298}{}^{Sol} = -80.31$ kJ/mol), the calculated energy values of EtP5@CPON ($\Delta H_{298}{}^{Sol} = -25.88$ kJ/mol, $\Delta G_{298}{}^{Sol} = -3.21$ kJ/mol) and EtP5@CHON ($\Delta H_{298}{}^{Sol} = -25.21$ kJ/mol, $\Delta G_{298}{}^{Sol} = -4.00$ kJ/mol) were relatively high, which led to the unstable structures of host-guest complexes (Table 2).

Considering that EtP6β exhibited excellent separation efficiency in the solid-vapor adsorption of alicyclic ketones and alicyclic alcohols, we wondered if EtP6β could also separate the liquid mixture of alicyclic ketones and alicyclic alcohols. Therefore, a solid-liquid adsorption experiment for the liquid mixture of CPOL and CPON (v:v = 1:1) by EtP6β was implemented. It was found that the adsorption amount of CPON liquid increased with time and reached two CPON molecules per EtP6 after 4 h, while that of CPOL liquid was negligible (Fig. 6a, Figs. S39 and S40 in Supporting information). Besides, the PXRD pattern of EtP6β after adsorbing the liq-

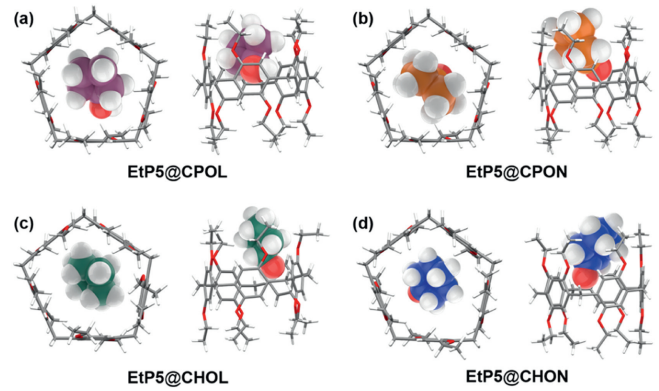

Fig. 5. Top and side views of DFT-optimized structures of (a) EtP5@CPOL; (b) EtP5@CPON; (c) EtP5@CHOL; (d) EtP5@CHON.

Table 2
Thermodynamic parameters of EtP5@CPOL, EtP5@CPON, EtP5@CHOL and EtP5@CHON at 298 K.

Sample	$\Delta H_{298}{}^{Sol}$ (kJ/mol)	$\Delta G_{298}{}^{Sol}$ (kJ/mol)
EtP5@CPOL	−24.72	−2.98
EtP5@CPON	−25.88	−3.21
EtP5@CHOL	−22.12	−3.85
EtP5@CHON	−25.21	−4.00

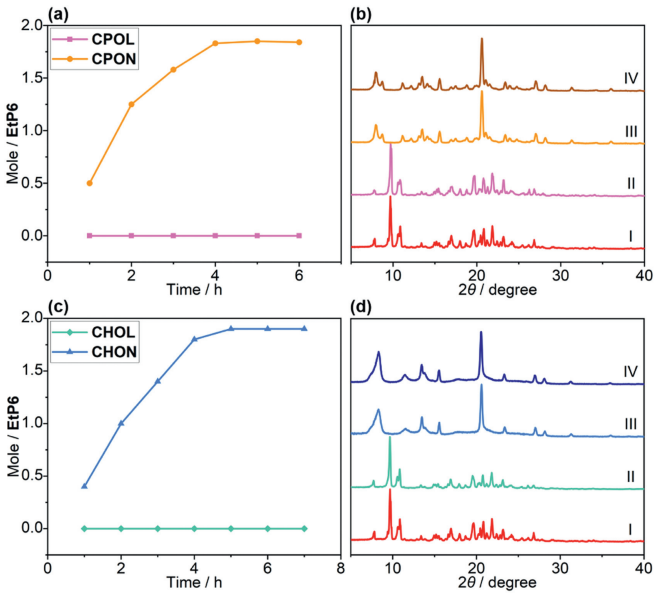

Fig. 6. (a) Time-dependent solid-liquid adsorption plots of EtP6β for the liquid mixture of CPOL and CPON (v:v = 1:1). (b) PXRD patterns of EtP6β: (I) original EtP6β; (II) after adsorption of CPOL liquid; (III) after adsorption of CPON liquid; (IV) after adsorption of the liquid mixture of CPOL and CPON (v:v = 1:1). (c) Time-dependent solid-liquid adsorption plots of EtP6β for the liquid mixture of CHOL and CHON (v:v = 1:1). (d) PXRD patterns of EtP6β: (I) original EtP6β; (II) after adsorption of CHOL liquid; (III) after adsorption of CHON liquid; (IV) after adsorption of the liquid mixture of CHOL and CHON (v:v = 1:1).

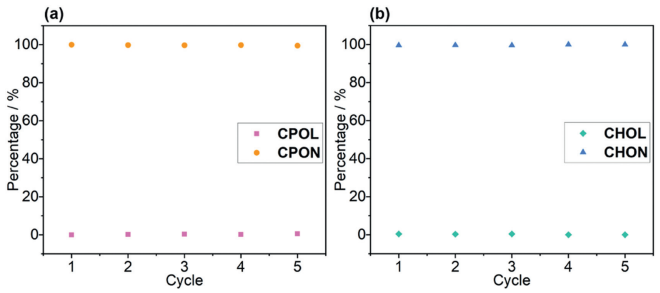

Fig. 7. Relative uptakes of (a) CPOL and CPON, (b) CHOL and CHON by EtP6β after 5 cycles.

uid mixture of CPOL and CPON was almost the same as that of EtP6β upon absorption of CPON liquid alone (Fig. 6b and Fig. S41 in Supporting information). These results revealed that EtP6β had the ability to selectively adsorb CPON from the liquid mixture of CPOL and CPON.

Similarly, the time-dependent solid-liquid adsorption experiment of EtP6β for the liquid mixture of CHOL and CHON (v:v = 1:1) was also conducted. The adsorption of CHON liquid by EtP6β increased over time and reached the saturation point after 5 h (Fig. 6c, Figs. S42 and S43 in Supporting information). But the adsorption amount of CHOL liquid by EtP6β was negligible. The PXRD pattern of EtP6β changed significantly after the uptake of CHON liquid, while that of EtP6β did not change after the uptake of CHOL liquid (Fig. 6d and Fig. S44 in Supporting information). In addition, the PXRD pattern of EtP6β after adsorption of the liquid mixture of CHOL and CHON was consistent with that of EtP6β after adsorption of CHON liquid alone. These results indicated that EtP6β exhibited excellent performance in the solid-liquid separation of CHON from the liquid mixture of CHOL and CHON.

In practical production, recycling performance is a crucial parameter [66–68]. Therefore, recycling adsorption experiments were conducted to investigate the recyclability of EtP6β. The EtP6@2CPON and EtP6@2CHON powders were heated under vacuum at 120 °C for 5 h to remove the loaded guests CPON and CHON from EtP6β. In addition, the newly formed EtP6 crystals were determined to be EtP6β by ^{1}H NMR (Figs. S45 and S46 in Supporting information) and PXRD (Figs. S47 and S48 in Supporting information). The resulting EtP6β powders were able to be reused and maintained their selectivity for CPON and CHON after 5 cycles without loss of performance (Figs. 7a and b).

In summary, for the first time, we developed a new method for the highly selective separation of equal-volume alicyclic ketone and alicyclic alcohol mixtures through NACs of EtP5 and EtP6 (EtP5α and EtP6β). It was found that EtP6β could separate CPON from the vapor mixture of CPOL and CPON (v:v = 1:1) as well as CHON from the vapor mixture of CHON and CHOL (v:v = 1:1) with purities of 99.1% and 100%, respectively, indicating that EtP6β were outstanding absorbents for the separation of alicyclic ketones and alicyclic alcohols. However, the adsorption of CPOL, CPON, CHOL and CHON by EtP5α was negligible. The DFT-optimized structures showed that the selectivity came from the thermodynamic stability of the newly formed crystal structures after adsorption of CPON and CHON molecules. Additionally, EtP6β were recyclable due to the reversible transformations between the guest-free structures and the guest-loaded structures. Therefore, EtP6β show tremendous potential as adsorbents to separate alicyclic ketones and alicyclic alcohols because of the advantages of simple synthesis, remarkable selectivity and high recyclability. Future investigations will concentrate on some of the more challenging separations, such as furfuryl alcohol/furfural and acetophenone/phenethyl alcohol.

Declaration of competing interest

The authors declare that they have no known competing financial interests or personal relationships that could have appeared to influence the work reported in this paper.

CRediT authorship contribution statement

Jingyu Chen: Writing – original draft. **Sha Wu:** Writing – original draft. **Yuhao Wang:** Investigation. **Jiong Zhou:** Writing – review & editing.

Acknowledgments

This work was supported by the National Natural Science Foundation of China (No. 22101043), the Fundamental Research Funds for the Central Universities (Nos. N2205013, N232410019, N2405013), Natural Science Foundation of Liaoning Province (No. 2023-MSBA-068), the Opening Fund of State Key Laboratory of Heavy Oil Processing (No. SKLHOP202203006) and Northeastern University. Special thanks are due to the instrumental or data analysis from Analytical and Testing Center, Northeastern University.

Supplementary materials

Supplementary material associated with this article can be found, in the online version, at doi:10.1016/j.cclet.2024.110102.

References

[1] Y. Wang, S. Sang, W. Zhu, L. Gao, G. Xiao, Chem. Eng. J. 299 (2016) 104–111.
[2] Q. Deng, R. Gao, X. Li, et al., ACS Catal. 10 (2020) 7355–7366.
[3] H. Liu, T. Jiang, B. Han, S. Liang, Y. Zhou, Science 326 (2009) 1250–1252.
[4] H. Yao, Y.M. Wang, M. Quan, et al., Angew. Chem. Int. Ed. 59 (2020) 19945–19950.
[5] B. Li, Y. Wang, L. Liu, M. Dong, C. Li, JACS Au 3 (2023) 1590–1595.
[6] T. Qiu, C.H. Kuang, C.G. Li, X.W. Zhang, X.D. Wang, Ind. Eng. Chem. Res. 52 (2013) 8139–8148.
[7] D.S. Sholl, R.P. Lively, Nature 532 (2016) 435–437.
[8] Y. Zhao, H. Xiao, C.H. Tung, L.Z. Wu, H. Cong, Chem. Sci. 12 (2021) 15528–15532.
[9] H. Chen, J. Sun, J. Ind. Eng. Chem. 94 (2021) 78–91.
[10] J. Qin, Q. Ye, X. Xiong, N. Li, Ind. Eng. Chem. Res. 52 (2013) 10754–10766.
[11] X.N. Han, Y. Han, C.F. Chen, Chem. Soc. Rev. 52 (2023) 3265–3298.
[12] A. Kirchon, L. Feng, H. Drake, E. Joseph, H.C. Zhou, Chem. Soc. Rev. 47 (2018) 8611–8638.
[13] D. Zhang, T.K. Ronson, R. Lavendomme, J.R. Nitschke, J. Am. Chem. Soc. 141 (2019) 18949–18953.
[14] D. Zhang, T.K. Ronson, Y.Q. Zou, J.R. Nitschke, Nat. Rev. Chem. 5 (2021) 168–182.
[15] A.P. Côté, A.I. Benin, N.W. Ockwig, et al., Science 310 (2005) 1166–1170.
[16] J.R. Li, J. Sculley, H.C. Zhou, Chem. Rev. 112 (2012) 869–932.
[17] X. Ma, P. Kumar, N. Mittal, et al., Science 361 (2018) 1008–1011.
[18] W.G. Cui, T.L. Hu, X.H. Bu, Adv. Mater. 32 (2020) 1806445.
[19] J. Liu, G. Han, D. Zhao, et al., Sci. Adv. 6 (2020) eabb1110.
[20] X. Li, N. Wang, X. Bao, et al., J. Mater. Chem. A 8 (2020) 17212–17218.
[21] Y. Wu, B.M. Weckhuysen, Angew. Chem. Int. Ed. 60 (2021) 18930–18949.
[22] L.K. Macreadie, O.T. Qazvini, R. Babarao, ACS Appl. Mater. Interfaces 13 (2021) 30885–30890.
[23] F. Xie, H. Wang, J. Li, Matter 5 (2022) 2516–2518.
[24] C.S. Smoljan, Z. Li, H. Xie, et al., J. Am. Chem. Soc. 145 (2023) 6434–6441.
[25] J. Wang, Y. Fan, J. Jiang, et al., Angew. Chem. Int. Ed. 62 (2023) e202304734.
[26] T. Rodenas, I. Luz, G. Prieto, et al., Nat. Mater. 14 (2015) 48–55.
[27] O.T. Qazvini, R. Babarao, Z.L. Shi, Y.B. Zhang, S.G. Telfer, J. Am. Chem. Soc. 141 (2019) 5014–5020.
[28] J. Zhou, G. Yu, Q. Li, M. Wang, F. Huang, J. Am. Chem. Soc. 142 (2020) 2228–2232.
[29] A. Dey, S. Chand, B. Maity, et al., J. Am. Chem. Soc. 143 (2021) 4090–4094.
[30] M. Yan, Y. Wang, J. Chen, J. Zhou, Chem. Soc. Rev. 52 (2023) 6075–6119.
[31] M. Yan, Y. Wang, J. Zhou, Cell Rep. Phys. Sci. 4 (2023) 101637.
[32] J. Yang, X.Y. Lou, D. Dai, J. Shi, Y.W. Yang, Chin. Chem. Lett. 36 (2025) 109818.
[33] T. Xiao, L. Zhou, L. Xu, et al., Chin. Chem. Lett. 30 (2019) 271–276.
[34] M. Yan, J. Zhou, Sci. China Chem. 66 (2023) 613–614.
[35] W. Yang, W. Zhang, J. Chen, J. Zhou, Chin. Chem. Lett. 35 (2024) 108740.
[36] T. Xiao, L. Qi, W. Zhong, et al., Mater. Chem. Front. 3 (2019) 1973–1993.
[37] Z.Q. Wang, X. Wang, Y.W. Yang, Adv. Mater. 36 (2024) 2301721.
[38] Y. Zhou, H. Tang, H. Wu, et al., Chin. Chem. Lett. 35 (2024) 108626.

[39] M. Ni, N. Zhang, W. Xia, et al., J. Am. Chem. Soc. 138 (2016) 6643–6649.
[40] Z. Wu, H. Qian, X. Li, T. Xiao, L. Wang, Chin. Chem. Lett. 35 (2024) 108829.
[41] Y. Li, X. Lou, C. Wang, et al., Chin. Chem. Lett. 34 (2023) 107877.
[42] J. Zhou, G. Yu, F. Huang, Chem. Soc. Rev. 46 (2017) 7021–7053.
[43] T. Xiao, W. Zhong, L. Zhou, Chin. Chem. Lett. 30 (2019) 31–36.
[44] J. Zhou, L. Rao, G. Yu, et al., Chem. Soc. Rev. 50 (2021) 2839–2891.
[45] T. Chen, J. Wang, R. Tang, et al., Chin. Chem. Lett. 34 (2023) 108088.
[46] M. Yan, S. Wu, Y. Wang, et al., Adv. Mater. 36 (2024) 2304249.
[47] F. Gao, X. Yu, L. Liu, et al., Chin. Chem. Lett. 34 (2023) 107558.
[48] T. Xiao, L. Zhang, D. Chen, et al., Org. Chem. Front. 10 (2023) 3245–3251.
[49] K. Jie, Y. Zhou, E. Li, F. Huang, Acc. Chem. Res. 51 (2018) 2064–2072.
[50] M. Wang, Q. Li, E. Li, et al., Angew. Chem. Int. Ed. 60 (2021) 8115–8120.
[51] M. Wang, S. Fang, S. Yang, et al., Mater. Today Chem. 24 (2022) 100919.
[52] Y. Wang, K. Xu, B. Li, et al., Angew. Chem. Int. Ed. 58 (2019) 10281–10284.
[53] J.R. Wu, Y.W. Yang, J. Am. Chem. Soc. 141 (2019) 12280–12287.
[54] M. Liu, R. Cen, J. Li, et al., Angew. Chem. Int. Ed. 61 (2022) e202207209.
[55] S.Y. Li, H. Yao, H. Hu, et al., Chem. Commun. 59 (2023) 7204–7207.
[56] J.R. Wu, G. Wu, Y.W. Yang, Acc. Chem. Res. 55 (2022) 3191–3204.
[57] N. Song, T. Kakuta, T.A. Yamagishi, Y.W. Yang, T. Ogoshi, Chem 4 (2018) 2029–2053.
[58] J.R. Wu, B. Li, Y.W. Yang, Angew. Chem. Int. Ed. 59 (2020) 2251–2255.
[59] Y. Wang, S. Wu, S. Wei, Z. Wang, J. Zhou, Chem. Mater. 36 (2024) 1631–1638.
[60] J. Chen, W. Zhang, W. Yang, et al., Nat. Commun. 15 (2024) 1260.
[61] X. Xu, V.V. Jerca, R. Hoogenboom, Angew. Chem. Int. Ed. 59 (2020) 6314–6316.
[62] X. Zhang, X. Wang, B. Wang, Z.J. Ding, C. Li, Chin. Chem. Lett. 31 (2020) 3230–3232.
[63] J.R. Wu, G. Wu, D. Li, D. Dai, Y.W. Yang, Sci. Adv. 8 (2022) 2255.
[64] G. Zhang, W. Lin, F. Huang, J. Sessler, N.M. Khashab, J. Am. Chem. Soc. 145 (2023) 19143–19163.
[65] M. Wang, J. Zhou, E. Li, et al., J. Am. Chem. Soc. 141 (2019) 17102–17106.
[66] P.F. Cui, X.R. Liu, Y.J. Lin, Z.H. Li, G.X. Jin, J. Am. Chem. Soc. 144 (2022) 6558–6565.
[67] K. Cheng, H. Li, Z. Li, P.Z. Li, Y. Zhao, ACS Mater. Lett. 5 (2023) 1546–1555.
[68] Y. Wang, Z. Wang, S. Wei, et al., Mater. Chem. Front. 8 (2024) 2273–2281.